



UNIVERSITÉ  
LAVAL

# Modeling the Breakdown in Degeneracy for High-Index-Contrast Ring Core Fiber

Mai Banawan, Lixian Wang, Sophie LaRochelle, and Leslie A. Rusch

IEEE/OSA Optical Fiber Communications Conference (OFC 2020)

© 2020 IEEE/OSA. Personal use of this material is permitted. Permission from IEEE/OSA must be obtained for all other uses, in any current or future media, including reprinting/republishing this material for advertising or promotional purposes, creating new collective works, for resale or redistribution to servers or lists, or reuse of any copyrighted component of this work in other works.

# Modeling the Breakdown in Degeneracy for High-Index-Contrast Ring Core Fiber

Mai Banawan<sup>1</sup>, Lixian Wang<sup>2</sup>, Sophie LaRochelle<sup>1</sup>, and Leslie A. Rusch<sup>1\*</sup>

<sup>1</sup>Department of Electrical and Computer Engineering, COPL, Université Laval, Québec, Canada

<sup>2</sup>Huawei Technologies Canada Co., Ltd., ON, Canada

\*rusch@gel.ulaval.ca

**Abstract:** Our numerical model of elliptical deformation of ring cores uncovers distinctly different behaviors of lower and higher order OAM modes. Degeneracy of modes, across topological charge and polarization are laid bare in simulations. © 2020 The Author(s)

**OCIS codes:** 060.2270, 060.2310, 060.2400.

## 1. Introduction

Orbital angular momentum (OAM) modes are under study as they require no or low ( $2 \times 2$ ) multiple input multiple output (MIMO) digital signal processing (DSP) for data multiplexing [1]. In [2], degeneracy among OAM mode pairs was predicted for lower order modes due to ellipticity in the guiding ring core. At higher modes (order 5 and above), MIMO-free transmission (i.e., with lifted degeneracy) was observed experimentally [3]. A numerical model, similar to that for linearly polarized modes in few mode fibers, was used for OAM modes in strongly guiding fibers in [4]. The model did not address the degeneracy issue nor other coupling behaviors that vary with the mode order. We need an accurate model to describe and quantify the coupling mechanism in OAM fibers to better design mode multiplexing systems (from fibers to receivers).

In this paper, we introduce a new method to find the coupling strength between OAM modes under elliptical deformation of the fiber core. Unlike the traditional approach based on first order perturbation [4, 5], we exploit numerical mode solver outputs of perturbation and show improved predictions in coupling. Only the new technique finds the coupling between degenerate OAM mode pairs, and produces results for near-degenerate pairs and other neighboring modes that echo experimental observations (less coupling between OAM mode pair at higher orders). For a given fiber design, our simulations predict the OAM order at which the degeneracy between OAM mode pair is lifted, leading to no crosstalk between opposite topological charges. Such knowledge will allow us to determine the most appropriate MIMO-DSP for a given fiber length and lead to better fiber design strategies.

## 2. Modal Equations

OAM modes can be described as a linear combination of fiber even and odd eigenmodes with circular polarization

$$OAM_{\pm l, m}^{\pm} = HE_{l+1, m}^e \pm iHE_{l+1, m}^o \quad \text{and} \quad OAM_{\pm l, m}^{\mp} = EH_{l-1, m}^e \pm iEH_{l-1, m}^o \quad (1)$$

where  $l$  is the mode topological charge,  $m$  is the radial index and the superscripts  $+$  and  $-$  signs indicate right and left circular polarizations of the OAM mode respectively [2, 4]. The first two modes are a spin-orbit aligned (A) mode pair: the field phase front and polarization are in the same direction. The second two modes are an anti-aligned (AA) mode pair (opposite directions of phase front and polarization). In our notation  $(+)$ 4AA would be equivalent to OAM with topological charge of  $+4$  and left circular polarization, or  $OAM_{+4, 1}^-$ . A numerical mode solver is used, as in [6] for silicon arrayed waveguides, to find the mode coupling coefficients in the presence of a geometric deformation. The method exploits the mode profiles and propagation constants of the perturbed and unperturbed fibers obtained using a mode solver to solve a system of linear equations to find the coupling matrix.

In classical coupled-mode theory [7], the electric field of the perturbed eigenmodes  $\tilde{E}_v$  is related to the electric field of eigenmodes  $E_\mu$  of a perfectly circular ring by

$$\tilde{E}_v = \sum_{\mu=1}^{\infty} c_{\mu v}(z) E_\mu \quad (2)$$

where  $c_{\mu v}$  are the elements of the eigenvector of the  $v^{\text{th}}$  eigenmode; they vary with propagation distance  $z$ . The coupled mode equations (CMEs) of the  $v^{\text{th}}$  mode eigenvector during propagation are

$$\frac{dc_{vv}(z)}{dz} = i \left[ \beta_v c_{vv}(z) + \sum_{\mu=1}^{\infty} k_{v\mu} c_{\mu v}(z) \right] \quad (3)$$

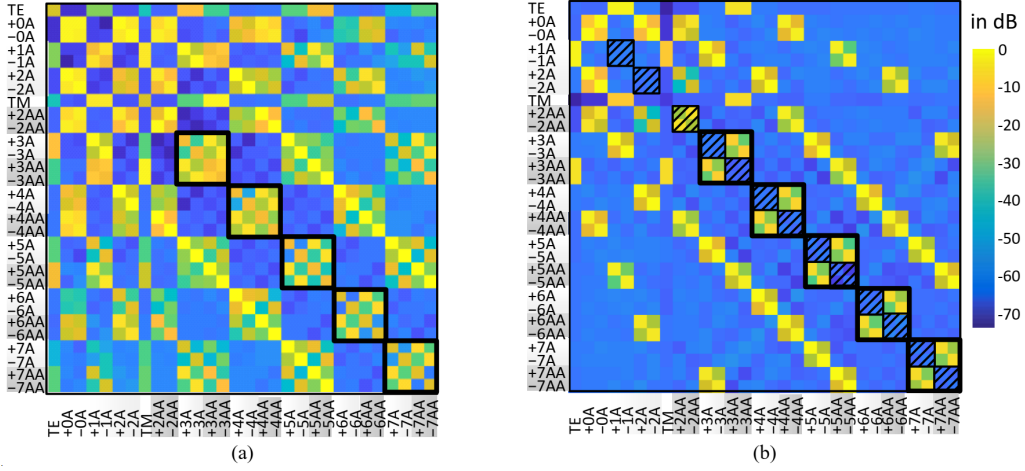


Fig. 1: Comparison between OAM coupling matrix  $\mathbf{K}_{OAM}$  in dB calculated (a) using numerical mode solver-based method and (b) using perturbation theory-based method from [4]. Coupling coefficients are normalized to the maximum value of 28 dB

where  $\beta_v$  is the propagation constant of the  $v^{th}$  unperturbed eigenmode. Assuming uniform ellipticity along the fiber,  $c_{vv}$  has a constant amplitude, and the phase dependence takes the form  $\exp(i\beta_v z)$ . CMEs can be written as

$$\left(\beta_v - \tilde{\beta}_v\right) c_{vv}(z) + \sum_{\mu=1}^{\infty} k_{v\mu} c_{\mu v}(z) = 0 \quad (4)$$

where  $\tilde{\beta}_v$  is the propagation constant of the  $v^{th}$  eigenmode in the perturbed fiber.

Defining  $\mathbf{B}$  as  $\text{diag}(\tilde{\beta}_1, \tilde{\beta}_2, \dots, \tilde{\beta}_N)$  and  $\mathbf{D}$  as  $\text{diag}(\beta_1, \beta_2, \dots, \beta_N)$  where  $N$  is the number of modes supported in the fiber, (4) can be written in matrix form as  $\mathbf{CB} = (\mathbf{D} + \mathbf{K})\mathbf{C}$ . We can change modal basis from the eigenmodes to the OAM modes, with  $\mathbf{K}_{OAM}$  being the new coupling matrix. According to (1) and (46) in [7], the coupling coefficients  $\kappa$  between two OAM mode pairs  $(v, v+1)$  and  $(\mu, \mu+1)$  couple when  $v$  and  $\mu$  are the even eigenmodes, via this transformation

$$\begin{bmatrix} \kappa_{v,\mu} \\ \kappa_{v,\mu+1} \\ \kappa_{v+1,\mu} \\ \kappa_{v+1,\mu+1} \end{bmatrix} = \begin{bmatrix} 1 & i & -i & 1 \\ 1 & i & i & -1 \\ 1 & -i & -i & -1 \\ 1 & -i & i & 1 \end{bmatrix} \begin{bmatrix} k_{v,\mu} \\ k_{v+1,\mu} \\ k_{v,\mu+1} \\ k_{v+1,\mu+1} \end{bmatrix} \quad (5)$$

Numerical manipulations are performed in the eigenmode basis; results are presented in the OAM modal basis.

### 3. Simulation Results

#### 3.1. Evaluation of Coupling Matrix

Elements of the coupling matrix  $\mathbf{K}$  can be evaluated via perturbation theory using an overlap integral as in [4, 7]. First the circular ring core is treated in COMSOL to yield mode electrical fields and their propagation constants (used to form  $\mathbf{D}$ ). An overlap integral of the electrical fields with a perturbative terms is used to determine  $\mathbf{K}$ .

In our new proposed method, both circular (unperturbed) and slightly elliptical (perturbed) fibers are simulated in COMSOL to extract mode electric fields; fiber material is isotropic. The elliptical deformation flattens the fiber cross-section along one axis. The eigenvectors over the fiber cross-section area are found via (2), yielding  $\mathbf{C}$ . Matrices  $\mathbf{B}$  and  $\mathbf{D}$  are found from the COMSOL output. Coupling coefficients,  $\mathbf{K}$  and  $\mathbf{K}_{OAM}$ , are found from (4) and (5) respectively. We simulate the hollow thin ring-core fiber designed in [8] and compare our results with the approach used in [4]. The fiber has four layers: air-core, ring-core, trench, and cladding with radii in  $\mu\text{m}$  of 9.1, 11.3, 16.2 and 25 respectively, and refractive indexes of 1, 1.474, 1.438 and 1.444 respectively.

The coupling matrix  $\mathbf{K}_{OAM}$  calculated using our proposed method at ellipticity of 1% is in Fig. 1(a), and results for the perturbation theory-based method in Fig. 1(b). Clearly the modal interactions are distinct in the new method, as the matrix comprises more coefficients. The most profound differences, however, can be seen in the  $4 \times 4$  sub-matrices along the diagonal with black outline for OAM orders 3-7. For both models, the anti-diagonal  $2 \times 2$  sub-matrices are non-zero. Patterned squares for  $2 \times 2$  sub-matrices in Fig. 1(b) recall that during simulation of propagation in fiber, these modes are assumed degenerate with the classical model [4]. In Fig. 1(a) same  $2 \times 2$  sub-matrices on the main diagonal are calculated in our new method, and can inform us on degeneracy; the two

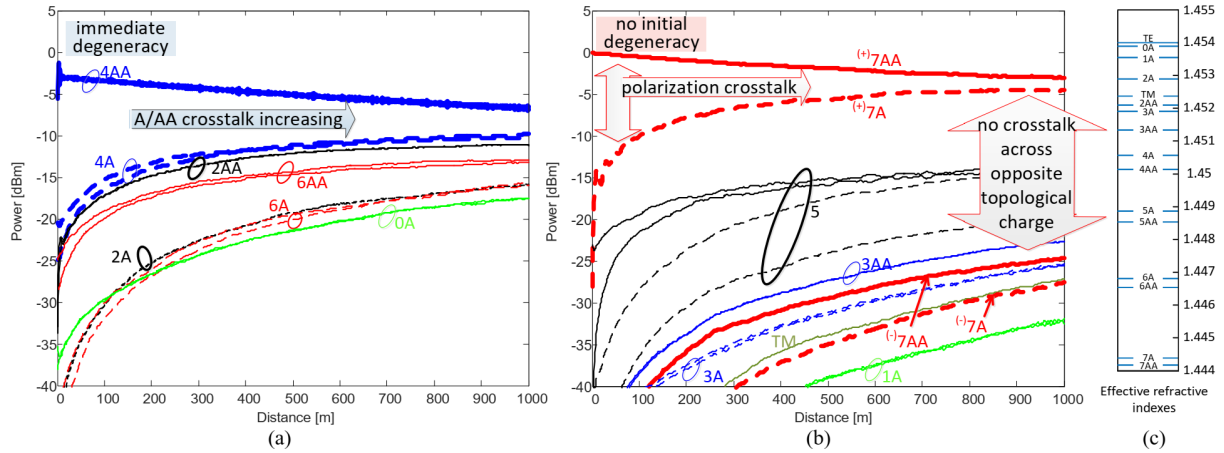


Fig. 2: Power evolution of OAM modes vs. transmission distance when launching (a) lower-order OAM<sup>(+)</sup>4AA, (b) higher-order OAM<sup>(+)</sup>7AA. Solid line for AA modes, dashed lines for A modes, value of topological charge is written beside curves and ovals surround one/two mode pairs. and (c) effective refractive indexes of OAM modes

anti-diagonal entries become zero if degeneracy is lifted (e.g. entry between <sup>+</sup>7A and <sup>-</sup>7A). Another significant difference between the two methods is the variation of these  $4 \times 4$  matrices across mode order. Contrast mode 3 and mode 7; the  $4 \times 4$  sub-matrices are almost identical in the classical model, and disparate in the new method.

Birefringence between the even (*e*) and odd (*o*) eigenmodes forming OAM mode, see (1), is induced by the elliptical deformation; in our method this birefringence is captured by **B** and influences **K**. In particular, this leads to non-zero coupling coefficients between the OAM mode pair and is the improvement offered by our method. Moreover, the detuning of the OAM mode pair (on the main diagonal) leads to spatial beating between them [5].

### 3.2. Numerical Propagation

To evaluate the mode propagation along the optical fiber by solving (3), random rotation of fiber principle axes must be taken into account. This effect can be captured by modeling the fiber as a concatenation of small fiber subsections, each subsection has a length below the fiber correlation length. The orientation angle of fiber axes changes from one section to another per a Wiener process - see the fixed modulus model in [2, 4]. The previously calculated coupling matrix will be transformed into the new rotated fiber axes as in [4]. For circularly polarized light, rotating fiber principle axes results only in a phase shift between mode pairs.

Figure 2 shows the power evolution of one launched OAM mode and the power leaked to the other modes during propagation along 1 km of the OAM fiber; the chosen fiber correlation length is 20 meters, close to the one measured in [2]. For lower mode order, as indicated in Fig. 2(a), the two AA modes of order 4 mixed immediately after very a few meters; DSP would be required to demultiplex these modes. Coupling between A and AA mode pairs increases with distance; this coupling also depends on the effective index separation between the two pairs, provided in Fig. 2(c), which is  $4.3 \times 10^{-4}$  for order 4.

For order 7, behavior changes significantly, as seen in Fig. 2(b) compared to Fig. 2(a). There is no initial degeneracy and the launched mode could be received with no MIMO for some distance. Coupling between opposite polarization and same topological charge (e.g., <sup>+</sup>7AA and <sup>+</sup>7A) is more significant than within the AA pair. This coupling across AA/A at 1 km is higher for order 7 than order 4, as order 7 has lower effective index separation.

## 4. Conclusion

Our modeling method predicts more precisely OAM mode coupling due to elliptical deformation. Compared to the perturbation-theory approach showing only coupling between different mode groups, our method uncovers coupling behavior within a mode pair. We predict lower order OAM modes need at least  $2 \times 2$  MIMO with short equalizers for propagation, while higher order modes could support MIMO-free transmission for a short distance.

## References

1. N. Bozinovic, et al., *Science*, 340(6140), 1545–1548, 2013.
2. L. Wang, et al., *J. of Lightwave Technology*, 34(8), 1661-1671, 2016.
3. K. Ingerslev, et al., *Optics Express*, 26(16), 20225, 2018.
4. G. Guerra, et al., *Optics Express*, 27(6), 8308-8326, 2019.
5. R. Ulrich, et al., *Applied Optics*, 18(13), 2241-2251, 1979.
6. M. L. Cooper, et al., *Optics Express*, 17(3), 1583-1599, 2009.
7. D. Marcuse, *The Bell System Technical Journal*, 54(6), 985-995, 1975.
8. C. Brunet, et al., *Optics Express*, 22(21), 26117-26127, 2014.